Some Research Results on Bridge Health Monitoring, Maintenance and Safety III

Edited by
Yang Liu

Some Research Results on Bridge Health Monitoring, Maintenance and Safety III

Special topic volume with invited peer reviewed papers only.

Edited by

Yang Liu

TTP

Preface

In China, the amount of deteriorating bridges is increasing gradually, and the costs of maintenance, repair and rehabilitation of these bridges far exceed available budgets. Internationally, above issue also is paid more attention. To alleviate this issue, the bridge engineering profession continues to take positive steps towards developing more comprehensive bridge monitoring and management systems. Therefore, it is significant to combine some good works that have been done in this field, which is the original objective to introduce the recent research results in the fields of bridge health monitoring, bridge maintenance and safety in the mainland of China. This project encompasses some aspects of bridge health monitoring, maintenance and safety. Specifically, it deals with: bridge health monitoring; bridge repair and rehabilitation issues; bridge related safety and other implications.

Table of Contents

Cracking Control for Diaphragm of Long-Span Prestressed Concrete Box Girder Bridge at the Early Age

Guodong Li[1,a], Zonglin Wang[1,b]

[1]School of Transportation Science and Engineering, Harbin Institute of Technology, Harbin, China, 150090

[a]happy_liguodong@163.com, [b]wangzonglin@vip.163.com

Abstract: This paper presents the results of a study on the early-age cracking behavior of diaphragm in long-span prestressed concrete box girder bridge with cracking control techniques. Based on the three-dimensional hydration heat temperature conduction and humidity diffusion theory, and according to the similarity of differential equation between the humidity diffusion theory and temperature conduction theory, the early-age cracking of diaphragm was simulated by a three-dimensional finite element model with consideration of concrete shrinkage, creep, cement hydration heat and variation of temperature. The numerical simulation accurately predicts the cracking region and size and stress time history of diaphragm, and provides load standard for cracking control techniques of prestressing force. The cracking control techniques of prestressing force effectively avoid the early-age cracking of diaphragm by application of practical engineering.

1 Introduction

The diaphragm can increase the torsional stiffness of section, restrain sectional distortion, and improve the overall mechanical performance of bridge, which is an important part of long-span prestressed concrete box girder bridge. For the diaphragm located pivot point, if the support is under the web, it can effectively disperse bearing reaction of web and baseplate, and avoid to damage web by a overlarge counter-force; if the support is away from the web, it can directly deliver loads of superstructure to support, and become the main bearing component [1].

Obviously, to make the diaphragm to give full play to role must be ensured itself integrity. If the diaphragm cracks, it will not be able to provide sufficiently strength and stiffness to meet the requirement of bearing capacity. However, the diaphragm is often early cracking in actual engineering [2]. On the one hand, it does not attract the attention of design and construction control because the cracking cause of diaphragm is not very explicit, or some cracking factors were underestimated. On the other hand, although some cracking control measures were taken, there is not fundamental cracking control effect.

In this paper, the early-age cracking of diaphragm was simulated by a three-dimensional finite element model with consideration of concrete shrinkage, creep, cement hydration heat and variation of temperature based on the three-dimensional hydration heat temperature conduction and humidity diffusion theory, and analysis of the cracking mechanism. On this basis, the cracking control techniques of prestressing force to prevent the early-age cracking for diaphragm is discussed through the actual engineering.

2 The theory of temperature and humidity field

2.1 The theory of temperature field Based the hydration degree

The concrete satisfies the law of conservation of energy in the process of casting, and the heat conduction equation for three-dimensional unsteady temperature field of concrete can be constructed as equation (1).

$$\frac{\partial T}{\partial t} = D(t_e)\left[\frac{\partial^2 T}{\partial x^2} + \frac{\partial^2 T}{\partial y^2} + \frac{\partial^2 T}{\partial z^2}\right] + Q(a(t_e)) \tag{1}$$

Where,

$$a(t_e) = \frac{W_c(t)}{W_c^{tol}} = \exp\left(-\left(\frac{m}{t_e}\right)^n\right) \tag{2}$$

$$t_e = \int_0^t \exp\left[\frac{E}{R}\left[\frac{1}{T_r} - \frac{1}{T_a}\right]\right] dt \tag{3}$$

where $a(t_e)$ is the hydration degree at the age of t_e; $W_c(t)$ is the cumulative amount of cement in hydration reaction at the age of t; W_c^{tol} is the amount of cement; t_e is the equivalent time of Arrhenius equation; m, n is the content; T_r is the reference temperature, 293K; K is the chemical reaction rate; T_a is the reaction temperature, used absolute temperature; R is the gas constant, 8.315J/(mol·K); E is the activation energy; $D(t_e)$ is the thermal diffusivity of concrete at the equivalent time of t_e; $Q(a(t_e))$ is the output of heat.

The hydration degree is the degree of hydration reaction, and the hydration degree of some concrete mixture is showed as equation (2) in the certain reaction temperature [3-5], for a concrete mixture, as long as it has the same hydration degree, the physical properties should also be the same, and regardless of the curing temperature and age. This concept is similar to normality degree. In 1977, Freiesleben Hansen and Pedersen present the function of normality degree according to Arrhenius equation, which calculates the equivalent time of early-age concrete in the reference temperature, and is constructed as equation (3).

The temperature field is solved by finite element method after confirming the boundary and initial conditions. The transient heat transfer process is a system of heating or cooling process, in which temperature, heat flux boundary condition and internal energy are obviously variation over time, and the expression of the matrix form for its finite element equations is constructed as equation (4).

$$[C]\{\dot{T}\} + [K]\{T\} = \{Q\} \tag{4}$$

where $[K]$ is the conductance matrix consist of heat conductivity coefficient, convection coefficient, radiance and form factor; $[C]$ is the specific heat matrix; $\{T\}$ is the temperature vector of node; $\{\dot{T}\}$ is the derivative of temperature on time; $\{Q\}$ is the rate of heat flow vector of node.

2.2 The similarity of temperature field and humidity field on the differential equation

According to the form of control equation for temperature conduction and humidity diffusion in the differential field, it is showed as the tensor form in the equation (5), (6) which can more clearly compare their differences and relations.

$$D(\nabla^2 H_{,i}) + \dot{H}_{st} = \dot{H} \quad (i=1,2,3) \tag{5}$$

$$\eta(\nabla^2 T_{,i}) + \frac{1}{C_c \rho_c} \dot{Q}_t = \dot{T} \quad (i=1,2,3) \tag{6}$$

where ∇^2 is the laplace operator; $\dot{H}_{st}$ is the derivative of Wet source function on time; $\dot{Q}_t$ is the derivative of heat source function on time; $\dot{H}$ is the derivative of humidity on time; $\dot{T}$ is the derivative of temperature on time.

By comparing the two equations, it is shown that the form of both differential equations has the similarity; just their parameter values are different. It can be implemented by means of thermal analysis method to simulate the humidity field, so as to avoid the development of finite element analysis program for humidity diffusion.

3 Simulation and analysis of temperature and humidity field

3.1 The finite element model

There is the span of 2668.3 m in a bridge, and combination of span is 75 m + 2×125 m + 75 m in the main bridge. The diaphragm on top of pier is the thickness of 2.0m, the full height of 7.16m, the full width of 12.75m, the full height of 1.5m in the cave distance 1.8m from baseplate, and the width of 0.55m; the chamfer size is the 0.6m×0.3m (Fig. 1).

Fig.1 The appearance of the bridge

The modeling is used of ANSYS finite element analysis program in this paper showed in Fig.2, and the geometric model is set up by the actual design size in order to reduce calculation error. It is considered taken into account for the ordinary steel bar of diaphragm, prestressed steel bar of web, and horizontal prestressed steel bar of top plate in the model by separate modeling method (Fig.3). The steel bar is used of LINK 8 unit. The SOLID70 is used for thermal analysis, and the SOLID45 is used for structural calculation which is corresponding to each other. Thermal coupling analysis can be achieved by direct conversion unit thermal coupling analysis.
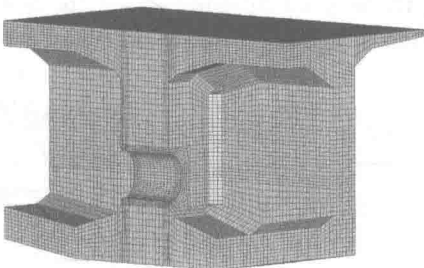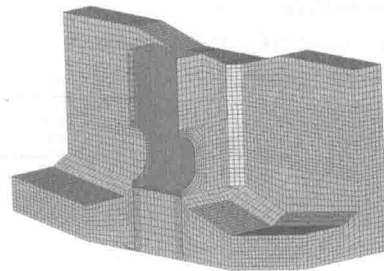

Fig.2 The model of diaphragm

Fig.3 The ordinary steel bar of diaphragm

3.2 The hydration heat temperature field of diaphragm

The three dimensional temperature field solutions are analyzed by hydration heat simulation model, to get the distribution of temperature field changing with time by the hydration heat, as shown in Fig.4.
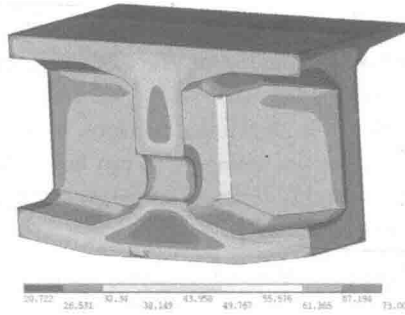

Fig.4 The distribution of hydration heat temperature field

The high temperature region and low temperature region of hydration heat are related to the local size and boundary conditions showed in Fig.4. General trend is that the size is the thick, the radiating surface the less, the greater the temperature rise. The cooling boundary around cave make temperature field above and below the cave to lose continuity, and there is the fastest area of temperature drop around the cave.

From the actual temperature control measures, it is easy to control from two aspects. The first is the size of the highest temperature rise inside. The second is the size of temperature gradient each layer. If the internal temperature rise is too high, it will cause a large tensile stress in the cooling stage. If the temperature gradient is too large, it will produce large tensile stress in the temperature rise and temperature drop stage.

3.3 Thermal stress of diaphragm

According to hydration heat temperature rise curve, the stress in the solution phase is divided into two parts, namely temperature rise stress and temperature drop stress. The superposition method is used for stress calculation; the calculated phase is divided into several periods showed as Equ. (7)[6].

$$\sigma_t = \sum_{i=1}^{n} \Delta\sigma_{t,i} \tag{7}$$

where,

$$\Delta\sigma_{t,i} = R_t \cdot \alpha_t \cdot \Delta T_{m,i} \cdot E_{e,i} \tag{8}$$

where R_i is the constraint degree of structure related to the concrete structure; α_t is the coefficient of linear expansion; $\Delta T_{m,i}$ is the time difference in temperature; $E_{e,I}$ is the average elastic modulus in the calculation time.

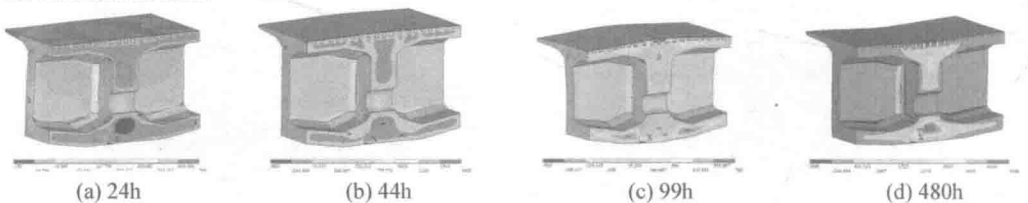(a) 24h   (b) 44h   (c) 99h   (d) 480h

Fig.5 The distribution of main tensile stress

There is the change of stresses in the temperature rise stage showed in Fig.5a, b; and the change of stresses in the temperature drop stage showed in Fig.5c, d. The stress state of diaphragm is the tension in the surface and the pressure interior because internal expansion strain is greater than the surface strain by temperature gradient. However, it is not produced a large stress because there is lower elasticity modulus of concrete that time, and principal tensile stress is showed in Fig.6.

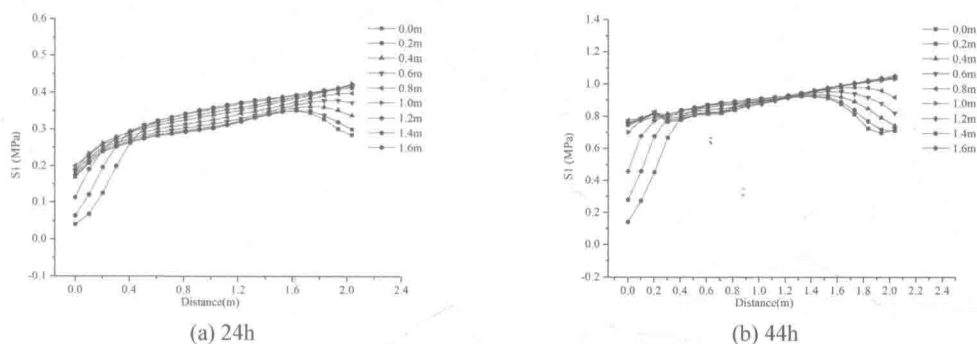(a) 24h   (b) 44h

Fig.6 The distribution of principal tensile stress in the surface

Family of curves presents the diagonal lines form in Fig.6. Because the casting pattern is the step by step up caused of tensile stress at the top of diaphragm lagging the tensile stress at the bottom. From casting to 24 hour, the principal tensile stress is about 0.4MPa, and to 44 hour, the principal tensile stress is about 1.1MPa.

(a) The principal tensile stress in the surface   (b) The principal tensile stress of the interior
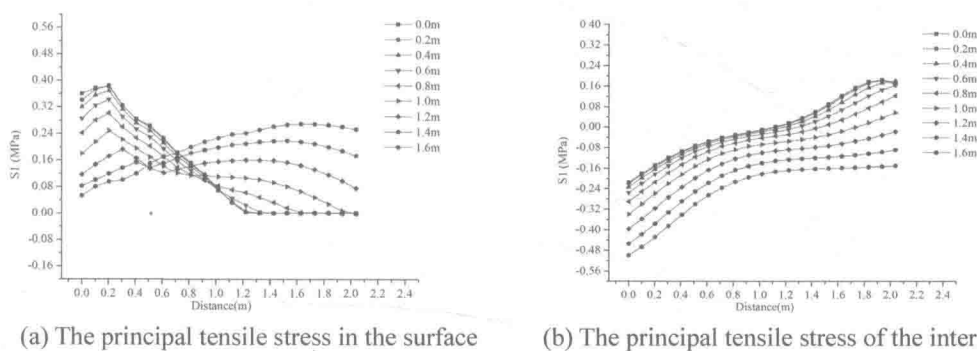
Fig.7 The distribution of principal tensile stress at the age of 96h

The principal tensile stress in the surface diaphragm integrally is decreased compared to it at the highest temperature at the age of 96h, and the bottom of diaphragm already presents tensile stress. Because the cooling at the top of cave is quicker than the near web, the tensile stress is reduced gradually from Y=0.0m to Y=1.6m showed in Fig.7.

It needs 20days to decrease the core temperature of diaphragm to the environment temperature by analog computation. The distribution of principal tensile stress at the age of 480h is shown in Fig.7. It does not present tensile stress in the surface of diaphragm after casting 20 days showed in Fig.7a, The tensional points in the curve are located inside the concrete. The cumulative tensile stress inside diaphragm is the relatively large in the cooling stage, and maldistribution shown as Fig.7b. Combining with the above results of temperature field analysis, the cooling is the fastest near cave

but the relatively slow at the position of baseplate, web and carrier plate. Different regions of diaphragm have different cooling time, it leads to the same temperature drop corresponding to different tensile stress in the development of elastic modulus of concrete over time, which can explain the distribution regularity of every curve in the Fig.7.
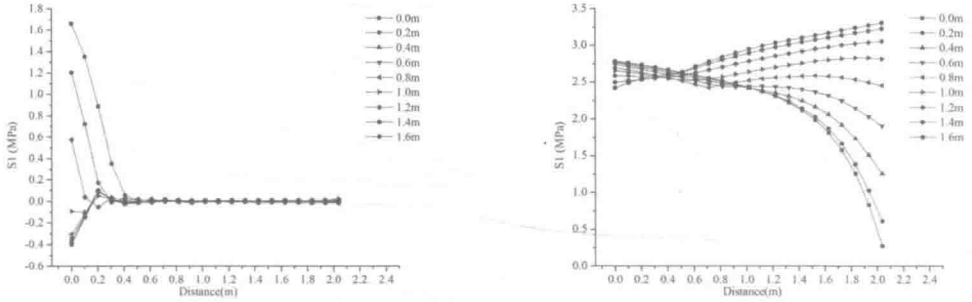
(a) The principal tensile stress in the surface   (b) The principal tensile stress of the interior

Fig.7 The distribution of principal tensile stress at the age of 480h

Comprehensive the above, the tensile stress diffusion path within diaphragm is fit for the overall trend from surface to interior, from bottom to top, and from the middle to web. Internal tensile stress at cooling stage is much larger than surface tensile stress at temperature rise stage; the cracking is more likely, once appearance of cracking, it is mostly connected crack, so it's more destructive.

3.4 The humidity field of diaphragm

The three dimensional humidity field solutions are analyzed by humidity simulation model, to get the distribution of humidity field changing with time, as shown in Fig.8.
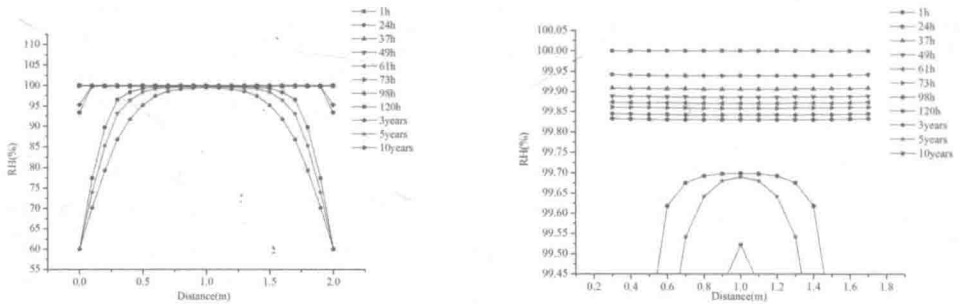
(a) The humidity distribution curve   (b) The effect of hydration reaction on humidity

Fig.8 The distribution of RH in the diaphragm

The process of gradual change of relative humidity (RH) over time in the thickness direction is showed in Fig.8. The desiccative area is considered between the above of each curve and RH=100%. The desiccative depth is almost zero from start to the first three days, and the surface of concrete starts desiccation to the fifth day decreased by 5%. As the extension of drying time, the desiccative area is more and more big, but the humidity gradient is smaller and smaller. In addition, the change of RH in boundary is obvious, and the change of RH in the middle diaphragm is not obvious over

time. The decrease of RH in the middle diaphragm is mainly derived from consuming humidity of hydration reaction, and not the impact of outside humidity diffusion. The effect of hydration reaction on RH is showed in Fig.8b.

The decreasing amplitude of RH in the first five days is accounts for 50% of the10 years' amounts, which illustrate that the early-age hydration thermal react rapidly, and about half of the amount of moisture dissipation is basically finished at the curing stage, which cause autogenous shrinkage deformation, and the early-age cracking [7,8].

3.5 The Shrinkage stress of diaphragm

It is discussed the distribution of normal stress over time for diaphragm. The contour liner of shrinkage stress at the early age is sowed in Fig.9. Contour is more intensive, the stress gradient the greater, otherwise, the stress gradient the smaller; the area surrounded by a contour is larger, the stress distribution more uniform, conversely, the stress concentration is more obvious.

(a) 3 day   (b) 9day   (c) 30 day
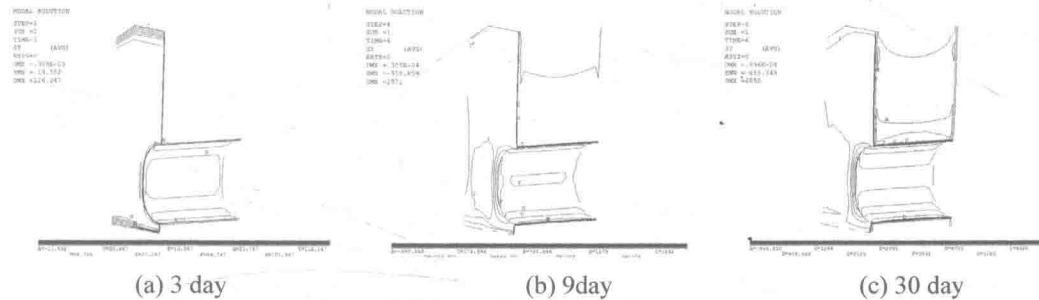
Fig.9 The contour liner of shrinkage stress at the early age

Combined with the humidity analysis results, Fig.9 is shown that the tensile stress is about 0.01 MPa on the third day (a week of curing period), to the 9th day (after two days of form removal), the tensile stress rises to about 1.5 MPa. Because surface humidity drops rapidly after form removal, the tensile stress rises to about 6.1 MPa to 30th day. For the range of tensile stress, the tensile stress on the surface of diaphragm is very small, mainly appears on the surface of cave, depth of no more than 3 cm. It indicates that the shrinkage stress of diaphragm is not synchronous and surrounding spread gradually from cave. But the early-age drying depth is shallow; the tensile stress is only on the surface [9, 10].

By the above analysis can draw the following conclusions, firstly, the shrinkage stress is not ignored stress field, and changing in time and space; secondly, the concrete has been in a state of shrinkage in tension at the scope of 2 cm within surface, it is obvious amplification of stress within one week after form removal, and maximizing after three weeks.

4 The cracking control techniques of prestressing force

The prestressing steel is arranged straight line in the diaphragm showed as Fig.10. Transverse prestressing steel is the steel cable of $13\phi15.2$; and vertical prestressing steel is the screw-thread steel bars of ϕ 32. The tension control stress under anchor is 1395MPa.The distribution of early-age stress after using prestressing force is showed in Fig. 11 by finite element method. To increase prestressing force can obviously increase prepressing stress of concrete in the diaphragm, Thus it can reduce the possibility of the early-age temperature and shrinkage cracking.
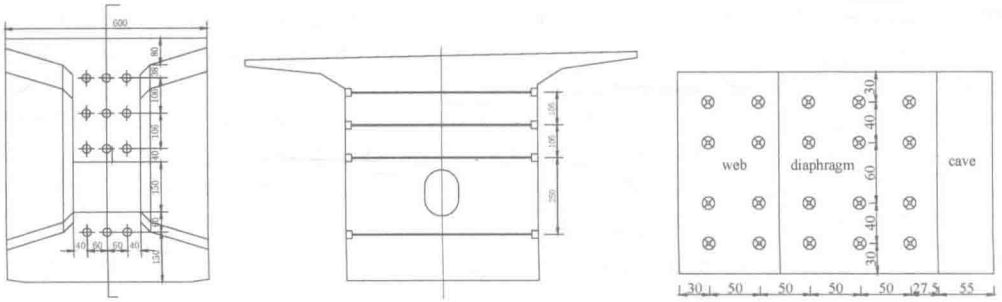
(a) The arrangement of Transverse prestressing   (b) The arrangement of vertical prestressing

Fig.10 The arrangement of prestressing force
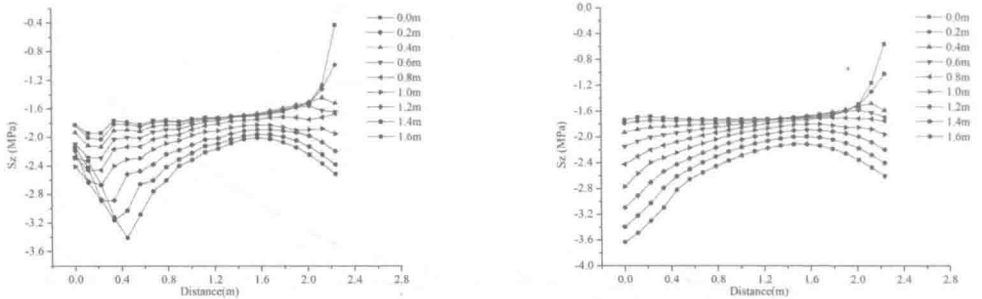
(a) The distribution of stress in the surface   (b) The distribution of stress in the middle

Fig.11 The distribution of stress after using prestressing force

It can make the concrete unit to appear the state of compression in advance by prestressing diaphragm, which decrease the tensile stress caused the early-age cracking of concrete, and make the concrete structure remain the state of compression or elastic working state. The cracking control technique of prestressing force is a kind of important measures to prevent diaphragm cracking, advantage of which is the targeted strong and easily to control load size [11]. Need to pay attention to the following matters when cracking control technique of prestressing force is used.

1. The transverse and vertical prestressing force should be arranged at the same time, and the vertical prestressing force should consider some more spare capacity to avoid transverse prestressing destruction of diaphragm later.

2. It should comply with vertical stretch-draw then transverse stretch-draw on the stretch-draw sequence, if, in turn, it is likely to be cracking phenomenon in the process of vertical stretch-draw.

3. It also can produce a certain longitudinal tensile stress in web when the vertical stretch-draw. If there are much vertical prestressing steel, not suitable to use one-off stretch-draw, and should combine with transverse stretch-draw. After several cantilever construction stage, construction loading (axial force) will be to provide a sufficient compressive stress in the position when it is filled the rest of prestressing force at this time. In the way, it not included with the destructive effect when applying prestressing force in all directions.

5 Conclusion

Based on the three-dimensional hydration heat temperature conduction and humidity diffusion theory, and according to the similarity of differential equation between the humidity diffusion theory and temperature conduction theory, the early-age cracking of diaphragm was simulated by a three-dimensional finite element model with consideration of concrete shrinkage, creep, cement hydration heat and variation of temperature in this paper.

1. The numerical simulation accurately predicts the cracking region and size, stress time history of diaphragm, and provides load standard for cracking control techniques of prestressing force.

2. The cracking control techniques of prestressing force effectively avoid the early-age cracking of diaphragm by application of practical engineering.

References

[1] C. S. Cai, Marico, Araujo *et al*. Diaphragm Effects of Prestressed Concrete Girder Bridges: Review and Discussion. ASCE, 161 (2007)1084~0680.

[2] Nam-Hoi Park, Nam-Hyoung Lim, Yong-jong Kang. A Consideration on Intermediate Diaphragm Spacing in Steel Box Girder Bridges with a Doubly Symmetric Section. Engineering Structures, 25 (2003)1665-1674.

[3] Enrique M, Antonio A. Distribution of Temperature and Stress in Concrete Box Girder Bridge. Journal of Structural Engineering, ASCE, 116(1990) 2388-2409.

[4] Moorty S, Roeder C W. Temperature Dependent Bridge Movements. Journal of Structural Engineering, ASCE, 118(1992)1090-1105.

[5] Elbadry M M, Ghali A. Temperature Variations in Concrete Bridges. Journal of Structural Engineering, ASCE, 109(1983)2355-2374.

[6] Roberts-Wollman C. L, Breen J. E, Cawrse J. Measurements of Thermal Gradients and Their Effects on Segmental Concrete Bridge. Journal of Bridge Engineering, 7(2002)166-174.

[7] T ARGO KALAMEES, MINNA KORPI. The Effects of Ventilation Systems and Building Fabric on the Stability of Indoor Temperature and Humidity in Finnish Detached Houses. Building and Environment, 44(2009)1643-1650.

[8] MEHRAN KH OSH BAKHT, MARKW LIN, JUSTINB BERMAN. Analysis of Moisture-Induced Stresses in FRP Composites Reinforced Masonry Structure. Finite Elements in Analysis and Design, 42(2006)414-429.

[9] N. J. Gardner. Comparison of Prediction Provisions for Drying Shrinkage and Creep of Normal-Strength Concretes. Canadian Journal of Civil Engineering, 31(2004)767-775.

[10]Francis T. K. AU, X. T. Si. Accurate Time-Dependent Analysis of Concrete Bridges Considering Concrete Creep, Concrete Shrinkage and Cable Relaxation. Engineering Structures, 33(2011)118-126.

[11]M. Saiidi, B. Douglas, S. Feng. Prestress Force Effect on Vibration Frequency of Concrete Bridges. Journal of structural engineering New York, N.Y, 120(1994)2233-2241.

Rapid Assessment Method of Girder Bridge Carrying Capacity Based on Traffic Running Test

Weizhao Li[1, a] , Xiaomin Huang[2,b] , Yan Li[3,c]

[1]Liaoning Provincial Bureau of communication Engineering Quality & Safety Supervision, Shenyang, China, 110005

[2]Department of Transport of Yunnan Province, Kunming, China,650031

[3]School of Transportation Science and Engineering, Harbin Institute of Technology, Harbin, China, 150090,

[a] lwzhit@163.com, [b] hjs.sy@163.com, [c] liyan_2007@126.com,

Keywords: Girder bridge, Traffic running test, Dynamic response, Low pass filter, Carrying capacity

Abstract. The dynamic response under running vehicle of the bridge includes the static response. The frequency components of simple supported beam dynamic response under the uniform constant force and the harmonic force were discussed. A method using the low pass filter to extract the static displacement from dynamic response curves was proposed and extended to the continuous girder bridge. Simulation analysis describes the process of extracting static displacement. The results show that the method is effective to separate the static and dynamic compositions from the vibration deflection. The dynamic deflection curves of an actual bridge was studied to get the generalized influence lines and then vehicles were laid on them as the static load test program to estimate the static deflection. The results of research show the estimative deflection has high precision and meets the requirements of the bridge inspection. This method can replace the static load test for rapid assessment of the girder bridge.

1 Introduction

People widely concerned how to timely master the bridge structure performance to ensure the safety of the operation because the bridge as an important transport hub. If the bridge management department can quickly and accurately assess the working status and safety performance of the existing bridge structure, then the maintenance and reinforcement measures may be reasonable and effective. Currently, the most widely used and relatively reliable assessment method for bridge is load test which divided into static load test and dynamic load test. In bridge structure experiment, the static load test is the mainly means of the bearing capacity evaluation, and the dynamic load test is in a secondary position which used for qualitative analysis of the structural state. Static load test method has mature testing technology and high precision of test data. But it has some disadvantages which making the application is limited such as the testing process is complex, testing time is long, need completely close bridge traffic.

In terms of application of dynamic test of bridge assessment, scholars at home and abroad have done corresponding research. Zhou Mi, He Shuanhai [1], Wang Feng [2] assessed the bearing capacity of a simply supported beam based on the inherent relationship of frequency and stiffness. Shi Zhou [3] systematically studied the bridge performance evaluation theory and application by means of structural damage identification based on the dynamic test. Lu, ZR, Law SS [4], Xu Weihua, Lv Zhongrong [5], Wang Shudong, Bu JianQing [6], Shan Deshan, Li Qiao[7] and other scholars researched bridge structure damage identification and evaluation theory based on the dynamic response under moving load. Bridge dynamic characteristics affected by the quality, the stiffness, boundary conditions of the bridge. The dynamic response is affected by characteristics and speed of vehicle and roughness of the bridge deck. If directly using them to assess structural stiffness, it is difficult to apply to the engineering practice. The response under moving vehicle of the bridge contains the static response. If the static response can be separated from all response, the method of static load experiment for bridge evaluation can be applied mechanically.